Angular differential cross sections for excitation of atomic hydrogen to the $n=2$ level by proton impact

J. T. Park, J. E. Aldag,* J. L. Peacher, and J. M. George†
Physics Department, University of Missouri-Rolla, Rolla, Missouri 65401
(Received 5 September 1979)

Differential cross sections for 15–145-keV proton impact excitation of atomic hydrogen to the $n=2$ level have been determined for center-of-mass scattering angles 0 to 1.2 mrad. The cross sections were obtained from an analysis of the angular distribution of protons which had lost an energy corresponding to the excitation of atomic hydrogen to its $n=2$ level. The differential cross sections obtained are in rather good agreement with available coupled-state calculations as well as the simpler Glauber-approximation calculations. However, at the larger scattering angles the cross sections obtained from the theoretical treatments appear to decrease more rapidly than the experimental data.

I. INTRODUCTION

The significance of ion-atom collisions in thermonuclear fusion, laser development, plasma diagnostics, and other critical areas has lead to a large number of theoretical calculations employing various approximations. The use of these approximate techniques for collision problems involving multielectron ions and atoms frequently involves additional approximations whose effect cannot be understood unless the effect of the primary approximations is understood. The primary tests of the initial approximations depend on the meager quantity of cross section data available for proton–atomic-hydrogen collisions. In spite of the fundamental importance of the proton–atomic-hydrogen cross section measurements, there have been relatively few experiments reported[1–10] for the excitation of atomic hydrogen by protons because of the experimental difficulties. Of these, only Park *et al.*[1–3] have reported cross sections for incident proton energies above 30 keV. Measurements of differential cross sections provide a better test of theoretical approximations than total cross sections because two different approximations could give similar results for total cross sections, but quite different results for cross sections differential in angle. However, the only previous differential measurements are the preliminary report of this measurement[1] and the measurement of Houver *et al.*,[5] who reported cross sections differential in angle for the excitation of atomic hydrogen to its $n=2$ level for proton impact energies of less than 2 keV.

The present experiment was designed to measure differential cross sections as a function of scattering angle for the collision process

$$H^+ + H(1s) \rightarrow H^+(\theta) + H(n=2)$$

for proton impact energies from 15 to 145 keV. This energy range covers the region where the total cross section for excitation of atomic hydrogen to its $n=2$ level reaches its maximum.

The University of Missouri-Rolla (UMR) ion-energy-loss spectrometer has been modified[1,11] to permit the measurements of differential cross sections for small-angle scattering of the projectile ion. The principle change involved placing the accelerator, beam alignment chamber, and target chamber on a platform that could be rotated about the collision point. The completed apparatus has an angular resolution of 37×10^{-6} rad which made possible the first measurement of this extremely basic differential cross section for excitation of atomic hydrogen from its ground state to its $n=2$ level by 15–145-keV incident protons.

II. EXPERIMENTAL METHOD

The energy-loss spectrometer and the general method employed in ion-energy-loss spectrometry have been discussed in detail elsewhere.[12–16] Several changes were made in the spectrometer[1,11] to permit measurement of accurate angular differential cross sections for atomic-hydrogen targets.

Ions are produced in a low-voltage discharge source. The ion source currently in use is a Colutron G2 Ion Gun, which includes a Wein filter to provide mass selection prior to acceleration. The energy distribution produced by this source is estimated to have a 0.2-eV full width at half maximum.

The mass-selected ions are accelerated and steered through the entrance collimator. The collimator slits can be moved precisely in and out of the beam. This makes it possible to focus the beam at the center of the collision chamber before introducing the collimator slits. This

method provides maximum beam intensity and also aids in data analysis. Additional collimation slits define the angular extent of the beam entering the collision chamber. The gas containment apertures of the collision chamber itself are larger than the maximum extent of the collimated beam and hence do not enter into the analysis of the collision geometry.

Ions exiting from the collision chamber pass through the exit collimator, which consists of a fixed exit slit and a pair of movable collimating slits. These slits are aligned for maximum transmission at zero scattering angle and define the detection window used in the data analysis.

The transmitted ion beam is magnetically analyzed to remove any products of charge-changing collisions. This removes any ambiguity as to the detected ion. Following the magnetic analysis, the ions enter the deceleration column and are decelerated by a well-defined potential. The decelerated ions are energy analyzed by an electrostatic analyzer.

A high-temperature furnace is used to produce atomic hydrogen. The target furnace is constructed of coaxial tungsten tubes, which are joule heated. Current flows radially into one end of the furnace, then flows coaxially through the tungsten furnace cylinder, returning through an adjacent coaxial shield, and lastly flowing radially outward. The proton beam is directed coaxially through the center of the furnace. Care is taken in the construction of the furnace in order to reduce any asymmetry in construction that might produce magnetic fields in the collision chamber.

Molecular hydrogen is dissociated into atomic hydrogen by a catalytic reaction involving a hot tungsten surface. Under the experimental conditions reported by Lockwood *et al.*,[17] it was possible to achieve a dissociation fraction of over 87.5% at a furnace temperature of 2380 K and still higher dissociation fractions at higher furnace temperatures. Both Lockwood's measurements and the measurements reported here were taken at molecular hydrogen pressures of the order of 10 mTorr. In this experiment the molecular hydrogen enters the region between the furnace wall and the heated coaxial shield. Because both the furnace wall and coaxial shield are at approximately 2700 K, the molecular hydrogen will be partially dissociated even before it diffuses through a small hole in the furnace into the scattering region.

The furnace is connected to a tube leading to a MKS Baratron Model 77 pressure meter. An automatic pressure regulator together with a servo-controlled valve maintains a constant furnace pressure using the Baratron pressure meter as a reference. The pressure difference from the setting on the Baratron pressure meter can be controlled to within 1% of the desired pressure.

In this experiment it is not necessary to accurately determine the percent of molecular hydrogen in the furnace because the 10.2-eV energy-loss peak in the spectra of atomic hydrogen is well resolved from the broad 12.5-eV energy-loss peak corresponding to the excitation of molecular states. With the target furnace cold, the energy-loss spectrum of molecular hydrogen is obtained when hydrogen gas is introduced into the target cell. The molecular-hydrogen spectrum displays a broad peak at 12.5 eV belonging to the Lyman-α bands. This spectrum starts at about 11.5-eV energy loss, reaches a peak at 12.5 eV, and decreases monotonically at higher energy losses. As the furnace is heated the spectrum begins to change. A 10.2-eV energy-loss peak that is attributed to the excitation of atomic hydrogen to its $n=2$ level appears. This peak increases while the peak at 12.5 eV changes shape and decreases.[3] During data acquisition the residual molecular hydrogen was less than 10% of the gas in the target furnace.

Spectra differential in energy loss are obtained by increasing the potential difference between the accelerator and decelerator terminals. Whenever the increased potential energy compensates for a discrete energy loss of the projectile-target system, a peak is detected in the energy-loss spectrum. The energy-loss scale can be determined to an accuracy[13] of ± 0.03 eV. Angular distributions of the scattered ion current corresponding to a particular scattering process can be measured by setting the energy loss at the calculated value[11] while pivoting about the scattering center provided that the process is resolved in its energy-loss spectrum. The relative angular position of the accelerator is known to within 3.3×10^{-6} rad.

The energy lost by the incident proton consists of two parts: (i) the energy lost to produce the excitation and (ii) the recoil energy of the target atom. At the laboratory scattering angles employed in this experiment the energy lost by the proton deviates from the excitation energy by at most 0.06 eV.

Because of the complexity of the measurement and the magnitude of data required to produce meaningful results, a minicomputer controls the data acquisition process. The measurement scattering angle, recoil-corrected energy loss, count time, and various emergency and reset signals are set and monitored by a minicomputer. Because the computer can vary the measurement time with the observed count rate, little time is

wasted on measurements for which the signal-to-noise ratio is high. The transmitted ion current, energy loss, scattering angle, and scattering chamber pressure are recorded for each measurement. This information is channeled directly to or preset by the minicomputer which corrects the measurement for scattering chamber pressure deviations, instrument- and residual-gas-caused background, and normal incident beam drift. A standard deviation is calculated for each data point and the results are averaged, background corrected, compacted, and stored for further analysis. Apparent differential cross sections are calculated from measurements of transmitted proton current as a function of angle.[11]

Care was taken to ensure single-collision conditions for this experiment. The standard technique of checking the linearity of the plots of zero-angle apparent differential cross section versus scattering chamber pressure was used to establish that the data were acquired under single-collision conditions.

The raw data obtained using the technique described above were analyzed using the method described in detail in Ref. 11. This data-analysis program extracts the "real" differential cross section from the apparent differential cross section by analyzing the effects of geometrical factors and the angular distribution of the incident beam. The description of the method is quite involved and will not be repeated here.

III. DATA

Differential cross section data for excitation of atomic hydrogen to the $n=2$ level by proton impact are shown by the solid octagons in Fig. 1. Table I gives the numerical values of the differential cross sections and the random error. The error bars are a result of two processes. The largest contribution to the error at the small scattering angles comes from the data-analysis program. The largest changes between the "real" differential cross section and the apparent differential cross section occur near zero scattering angle. This angular region is also the most sensitive to small changes in the incident beam distribution. As the scattering angle increases, errors arising from the data analysis decrease. However, errors arising from the statistical uncertainty of the scattered proton count rate increase. For the largest angles measured, the proton count rate was the same size as the noise. This leads to large error bars at the large scattering angles. As a result of these two processes, the error bars are large at the small scattering angles, decrease in size at increasing angles, and finally become largest at large scattering angles. The error bars represent only random errors obtained from the

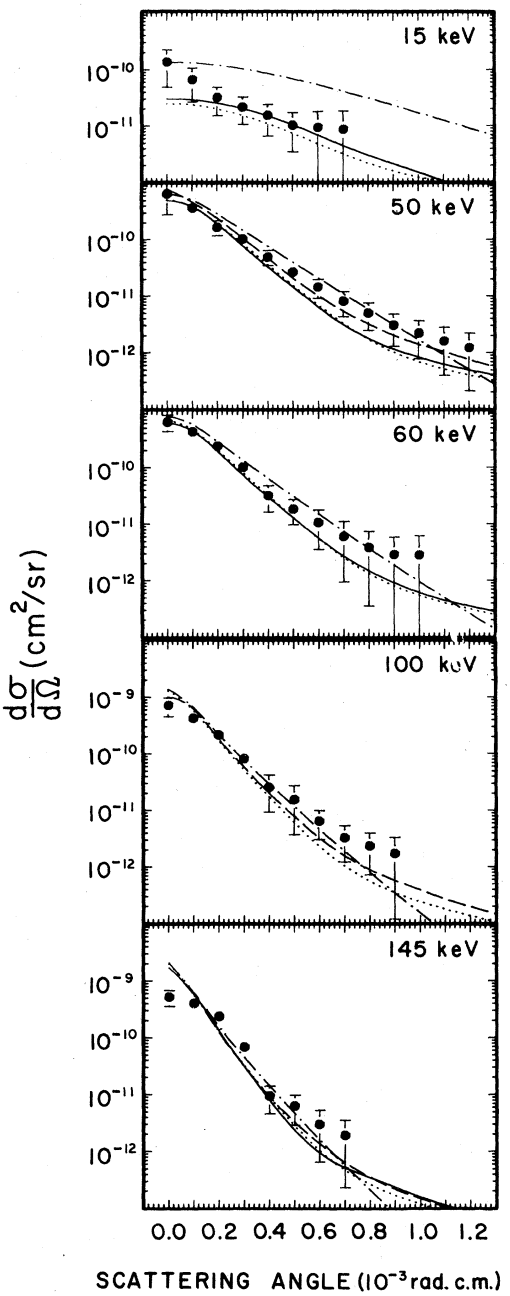

FIG. 1. Differential cross sections, in the center-of-mass frame, for the excitation of atomic hydrogen to the $n=2$ level by proton impact at selected lab energies. ●, present data; —·—, Born approximation (Refs. 32, 33); ·····, Glauber approximation (Refs. 32, 33); ——, scaled hydrogenic coupled-state calculation of Shakeshaft (Ref. 28); — — —, close-coupling pseudo-state calculation of Bransden and Noble (Ref. 29). Note that 150-keV results of Bransden and Noble have been plotted on the 145-keV graph.

TABLE I. Differential cross sections for excitation of atomic hydrogen to the $n = 2$ state by proton impact.

Angle (c.m.) (10^{-3} rad)	15 keV (cm^2/sr)	20 keV (cm^2/sr)	25 keV (cm^2/sr)
0.0	$(1.4\pm0.9)\times10^{-10}$	$(1.6\pm0.8)\times10^{-10}$	$(1.9\pm1.2)\times10^{-10}$
0.1	$(6.7\pm4.0)\times10^{-11}$	$(9.8\pm4.1)\times10^{-11}$	$(1.3\pm0.3)\times10^{-10}$
0.2	$(3.2\pm1.7)\times10^{-11}$	$(6.2\pm1.9)\times10^{-11}$	$(8.0\pm2.0)\times10^{-11}$
0.3	$(2.2\pm1.1)\times10^{-11}$	$(4.3\pm1.1)\times10^{-11}$	$(5.3\pm1.1)\times10^{-11}$
0.4	$(1.6\pm0.9)\times10^{-11}$	$(3.0\pm1.0)\times10^{-11}$	$(3.2\pm1.0)\times10^{-11}$
0.5	$(1.0\pm0.7)\times10^{-11}$	$(1.9\pm0.7)\times10^{-11}$	$(2.1\pm0.8)\times10^{-11}$
0.6	$(9.4\pm8.6)\times10^{-12}$	$(1.2\pm0.6)\times10^{-11}$	$(1.4\pm0.7)\times10^{-11}$
0.7	$(8.8\pm9.6)\times10^{-12}$	$(7.9\pm4.4)\times10^{-12}$	$(8.9\pm5.8)\times10^{-12}$
0.8		$(5.5\pm3.8)\times10^{-12}$	$(6.4\pm5.0)\times10^{-12}$
0.9		$(3.9\pm2.7)\times10^{-12}$	$(4.5\pm3.6)\times10^{-12}$
1.0		$(2.9\pm2.1)\times10^{-12}$	$(3.2\pm3.0)\times10^{-12}$
1.1		$(2.5\pm2.1)\times10^{-12}$	$(2.9\pm2.9)\times10^{-12}$
1.2		$(2.0\pm2.1)\times10^{-12}$	$(2.1\pm2.2)\times10^{-12}$

Angle (c.m.) (10^{-3} rad)	30 keV (cm^2/sr)	35 keV (cm^2/sr)	40 keV (cm^2/sr)
0.0	$(2.1\pm0.5)\times10^{-10}$	$(3.7\pm2.1)\times10^{-10}$	$(4.5\pm2.2)\times10^{-10}$
0.1	$(1.7\pm0.4)\times10^{-10}$	$(2.3\pm1.0)\times10^{-10}$	$(2.9\pm0.8)\times10^{-10}$
0.2	$(1.2\pm0.3)\times10^{-10}$	$(1.3\pm0.6)\times10^{-10}$	$(1.6\pm0.3)\times10^{-10}$
0.3	$(7.3\pm1.4)\times10^{-11}$	$(6.9\pm2.6)\times10^{-11}$	$(8.9\pm1.5)\times10^{-11}$
0.4	$(4.3\pm1.1)\times10^{-11}$	$(3.4\pm1.4)\times10^{-11}$	$(4.1\pm1.3)\times10^{-11}$
0.5	$(2.5\pm0.9)\times10^{-11}$	$(2.5\pm1.1)\times10^{-11}$	$(2.2\pm0.7)\times10^{-11}$
0.6	$(1.6\pm0.8)\times10^{-11}$	$(1.8\pm1.2)\times10^{-11}$	$(1.3\pm0.5)\times10^{-11}$
0.7	$(8.3\pm5.4)\times10^{-12}$	$(1.2\pm0.9)\times10^{-11}$	$(7.8\pm3.8)\times10^{-12}$
0.8	$(5.6\pm3.6)\times10^{-12}$	$(7.8\pm6.0)\times10^{-12}$	$(6.3\pm3.6)\times10^{-12}$
0.9	$(3.4\pm2.2)\times10^{-12}$	$(5.2\pm4.0)\times10^{-12}$	$(4.8\pm3.2)\times10^{-12}$
1.0	$(2.6\pm1.9)\times10^{-12}$	$(3.8\pm3.8)\times10^{-12}$	$(3.9\pm2.9)\times10^{-12}$
1.1	$(2.0\pm1.6)\times10^{-12}$	$(2.8\pm3.2)\times10^{-12}$	$(3.1\pm2.8)\times10^{-12}$
1.2	$(1.9\pm1.5)\times10^{-12}$	$(9.6\pm11.0)\times10^{-13}$	$(2.6\pm2.7)\times10^{-12}$

Angle (c.m.) (10^{-3} rad)	50 keV (cm^2/sr)	60 keV (cm^2/sr)	70 keV (cm^2/sr)
0.0	$(6.5\pm3.7)\times10^{-10}$	$(6.3\pm2.0)\times10^{-10}$	$(5.7\pm1.5)\times10^{-10}$
0.1	$(3.7\pm1.1)\times10^{-10}$	$(4.3\pm0.9)\times10^{-10}$	$(3.8\pm0.8)\times10^{-10}$
0.2	$(1.7\pm0.5)\times10^{-10}$	$(2.4\pm0.5)\times10^{-10}$	$(2.4\pm0.5)\times10^{-10}$
0.3	$(1.0\pm0.2)\times10^{-10}$	$(1.0\pm0.3)\times10^{-10}$	$(1.1\pm0.2)\times10^{-10}$
0.4	$(4.9\pm1.5)\times10^{-11}$	$(3.2\pm1.6)\times10^{-11}$	$(4.0\pm1.7)\times10^{-11}$
0.5	$(2.7\pm0.7)\times10^{-11}$	$(1.8\pm0.9)\times10^{-11}$	$(1.6\pm0.8)\times10^{-11}$
0.6	$(1.5\pm0.5)\times10^{-11}$	$(1.1\pm0.7)\times10^{-11}$	$(9.4\pm5.1)\times10^{-12}$
0.7	$(8.1\pm3.9)\times10^{-12}$	$(6.0\pm5.1)\times10^{-12}$	$(4.8\pm3.0)\times10^{-12}$
0.8	$(5.0\pm2.6)\times10^{-12}$	$(3.9\pm3.5)\times10^{-12}$	$(2.8\pm1.5)\times10^{-12}$
0.9	$(3.0\pm1.7)\times10^{-12}$	$(2.9\pm3.0)\times10^{-12}$	$(1.5\pm1.0)\times10^{-12}$
1.0	$(2.2\pm1.4)\times10^{-12}$	$(2.8\pm3.4)\times10^{-12}$	$(1.3\pm0.9)\times10^{-12}$
1.1	$(1.6\pm1.2)\times10^{-12}$		$(1.0\pm0.9)\times10^{-12}$
1.2	$(1.2\pm1.0)\times10^{-12}$		$(9.1\pm11.0)\times10^{-13}$

Angle (c.m.) (10^{-3} rad)	80 keV (cm^2/sr)	90 keV (cm^2/sr)	100 keV (cm^2/sr)
0.0	$(7.6\pm3.8)\times10^{-10}$	$(6.2\pm1.2)\times10^{-10}$	$(7.1\pm2.6)\times10^{-10}$
0.1	$(4.4\pm1.4)\times10^{-10}$	$(4.1\pm0.6)\times10^{-10}$	$(4.3\pm0.9)\times10^{-10}$
0.2	$(2.0\pm0.7)\times10^{-10}$	$(2.3\pm0.3)\times10^{-10}$	$(2.1\pm0.6)\times10^{-10}$
0.3	$(8.9\pm2.4)\times10^{-11}$	$(9.4\pm1.9)\times10^{-11}$	$(8.2\pm0.9)\times10^{-11}$
0.4	$(3.3\pm2.2)\times10^{-11}$	$(2.5\pm1.3)\times10^{-11}$	$(2.6\pm1.7)\times10^{-11}$
0.5	$(1.8\pm0.9)\times10^{-11}$	$(1.5\pm0.5)\times10^{-11}$	$(1.6\pm1.2)\times10^{-11}$
0.6	$(1.0\pm0.6)\times10^{-11}$	$(7.4\pm3.6)\times10^{-12}$	$(6.5\pm3.4)\times10^{-12}$
0.7	$(7.4\pm5.3)\times10^{-12}$	$(2.9\pm1.9)\times10^{-12}$	$(3.3\pm2.1)\times10^{-12}$

TABLE I. (*Continued*)

Angle (c.m.) (10^{-3} rad)	80 keV (cm^2/sr)	90 keV (cm^2/sr)	100 keV (cm^2/sr)
0.8	$(3.0\pm1.8)\times10^{-12}$	$(2.2\pm1.7)\times10^{-12}$	$(2.4\pm1.6)\times10^{-12}$
0.9	$(2.4\pm1.7)\times10^{-12}$	$(1.9\pm1.6)\times10^{-12}$	$(1.8\pm1.6)\times10^{-12}$
1.0	$(2.1\pm2.1)\times10^{-12}$		

Angle (c.m.) (10^{-3} rad)	125 keV (cm^2/sr)	145 keV (cm^2/sr)
0.0	$(6.3\pm2.3)\times10^{-10}$	$(5.2\pm1.7)\times10^{-10}$
0.1	$(4.0\pm1.1)\times10^{-10}$	$(4.0\pm0.8)\times10^{-10}$
0.2	$(2.0\pm0.5)\times10^{-10}$	$(2.4\pm0.5)\times10^{-10}$
0.3	$(8.5\pm2.3)\times10^{-11}$	$(6.9\pm1.8)\times10^{-11}$
0.4	$(2.4\pm2.0)\times10^{-11}$	$(9.4\pm4.8)\times10^{-12}$
0.5	$(1.2\pm0.9)\times10^{-11}$	$(6.3\pm3.5)\times10^{-12}$
0.6	$(4.9\pm4.1)\times10^{-12}$	$(3.0\pm2.3)\times10^{-12}$
0.7	$(2.2\pm1.5)\times10^{-12}$	$(1.9\pm1.7)\times10^{-12}$
0.8	$(1.7\pm1.4)\times10^{-12}$	
0.9	$(1.4\pm1.5)\times10^{-12}$	

combination of separate measurements and do not include any possible systematic errors arising from the apparatus, method of analysis, or from the method of normalization of the data.

Data were obtained during three different time periods separated by several weeks. For each time period, measurements were made using a new target furnace. There were no apparent systematic differences between data sets obtained from one time period to another.

Because the number density of atomic hydrogen in the furnace could not be accurately determined, the absolute values for the cross sections could not be directly obtained from the data. To obtain absolute cross sections the data are normalized. This normalization was accomplished by integrating the differential cross sections with respect to angle to obtain a total cross section at each incident energy. The total cross sections so obtained were then set equal to the total cross sections reported by Park *et al.*[2,3] Because the total cross sections reported by Park *et al.* are normalized to a first-Born-approximation calculation[18] at 200 keV, the differential cross sections reported here are thus normalized to a first-Born-approximation calculation of the total cross section for proton excitation of atomic hydrogen to its $n=2$ level at 200-keV incident proton energy.

IV. DISCUSSION

There are no other experiments reporting angular differential cross sections for the excitation of atomic hydrogen by proton impact for any part of the energy range reported in this paper. The only other experiment measuring angular differential cross sections for this collision system was published by Houver *et al.*,[5] which was for incident proton energies between 250 and 2000 eV.

Houver *et al.*[5] reported good agreement with the molecular expansion results of Chidichimo-Frank and Piacentini,[19] Knudson and Thorson,[20] and Gaussorgues *et al.*[21] However, the energy range of the incident protons in the experiment reported here is such that the collision is not expected to proceed primarily via molecular curve-crossing excitation mechanisms. For low-energy protons ($E<5$ keV), Chidichimo-Frank and Piacentini[19] reported that the dominant inelastic excitation is to the $2p_{\pm1}$ states of hydrogen. Excitation of the $n\geq3$ levels of atomic hydrogen should be weak. This report was substantiated by the absence of the $n\geq3$ energy-loss peaks in the spectra of Houver *et al.*[5] The energy-loss spectra obtained in the energy range covered by this experiment clearly demonstrate that the cross section for excitation of the $n\geq3$ levels are not orders of magnitude lower than the cross section for excitation of the $n=2$ level. This supports the belief that the mechanism for excitation in this experiment is different than the one in the experiment of Houver *et al.*[5]

As a further check for effects of molecular curve-crossing excitation mechanisms, plots of the reduced cross section, $\rho=\theta\sin\theta\, d\sigma/d\Omega$, versus $\tau=E\theta$ were made. However, the results did not lie on a universal curve. For the present data, the peak in the ρ value moves to lower τ values for decreasing proton energies, while the peak ob-

served by Houver *et al.*[5] is at a higher τ value. Thus the reduced cross section plot also supports the conclusion that molecular effects are not an important excitation mechanism in this experiment.

There are a number of theoretical coupled-state impact-parameter calculations for this system.[22-26] Unfortunately, there is no one-to-one correspondence between the scattering angle θ and the impact parameter b which is valid at these small angles.[27] Nevertheless, a small-angle classical calculation[27] was carried out using the static interaction potential for elastic scattering to obtain the relationship between θ and b. The experimental results obtained peaked at a lower impact parameter than the impact-parameter calculations, and agreement was poor.

Recently, Shakeshaft[28] and Bransden and Noble[29] have obtained differential cross sections from their coupled-state impact-parameter calculations. This is accomplished by multiplying the transition amplitudes at a given impact parameter by a suitable Bessel function and integrating over all impact parameters. Thus many impact parameters contribute to a given scattering angle. Shakeshaft[28] used a scaled hydrogenic basis set with 35 basis functions centered about each proton. The scale factors were chosen so that the resulting basis energy eigenvalues almost coincide with the energies of the $1s$, $2s$, $2p$, $3s$, $3p$, and $3d$ states and overlap the low-energy part of the continuous spectrum of the hydrogen atom. Bransden and Noble[29] used two sets of single-center expansions which included eigenfunctions to represent the discrete target states and pseudostates chosen to represent the continuum. Their basis set contained the exact $1s$, $2s$, and $2p$ hydrogenic wave functions. The first set, developed by Callaway and Wooten,[30] consists of five s, four p, and two d orbitals of the Slater type. The second set, first used by Callaway *et al.*,[31] is an extension of the first set and consists of seven s, five p, and three d orbitals. Both sets gave essentially the same results for the differential cross sections. Shakeshaft's[28] calculation gave good agreement with the experimental total excitation cross section of Park *et al.*[3] over the whole energy range, except for the region 40–70 keV in which his calculation takes a dip, whereas the experimental results go through a maximum. The Brandsen Noble[29] calculation gave good agreement with the experimental total excitation cross section of Park *et al.*[3] for energies above ~60 keV. Below about 60 keV their calculation yields a larger total excitation cross section than the experimental measurements.

The theoretical results of Shakeshaft for the differential cross section for direct excitation of the $n=2$ level is in reasonably good agreement with this experiment over the whole energy range measured from 15–145 keV. The agreement is quite good near 50 keV. The theoretical results of Bransden and Noble are also reasonably good over the energy range calculated, i.e., 50–150 keV. Their calculations do not extend below 50 keV because for energies less than 50 keV the total excitation cross section was being overestimated. These results are shown in Fig. 1.

Theoretical results of the first-Born- and Glauber-approximation calculations of Franco and Thomas[32] are also shown in Fig. 1. Thomas[33] very graciously provided the numerical values of these calculations.

The first-Born-approximation calculations give differential cross sections that are in fairly good agreement with the experimental cross section curve over all scattering angles measured for incident proton energies greater than 50 keV. For incident proton energies greater than 70 keV, the Born-approximation calculations yield results that are more sharply peaked with respect to angle than the experimental results. At the larger scattering angles the Born-approximation results have crossed over the experimental results so that the Born-approximation results are below the experimental results. After the Born-approximation results cross over the experimental results, they continue to decrease quite rapidly in magnitude as the scattering angle continues to increase.

Below incident proton energies of 40 keV, the first-Born-approximation calculations[32,33] yield differential cross sections that are larger than the experimental results for all angles. Also, the first-Born-approximation results are not falling as fast with respect to scattering angle as the experimental results. This is to be expected since the first-Born-approximation total cross sections are much higher than the experimental total cross sections in this energy range.[2,3]

The Glauber-approximation calculations[32,33] yield differential cross sections that are also in reasonably good agreement with the experimental differential cross sections over the entire range of incident proton energies reported here. The Glauber approximation does remarkably well considering its computational simplicity. It is interesting to note that the Glauber-approximation results for the differential cross section approach the experimental results from below, as do the Glauber-approximation results for the total $n=2$ excitation cross section.

The coupled-state calculations of Shakeshaft[28] and Bransden and Noble,[29] as well as the simpler Glauber-approximation calculation of Franco and

Thomas,[32] yield a curve shape for the differential cross section which is in reasonably good agreement with the experimental results for the angles measured. On the other hand, the first Born approximation does not have the correct curve shape for the differential cross section even though its magnitude is close to the experimental results for energies greater than 50 keV. All of the other theoretical treatments differ from the data slightly in curve shape. At zero scattering angle these theories are low compared to experiment at low energies, very good near 50 keV, and higher than experiment at higher energies. At the larger scattering angles the cross sections obtained from the theoretical treatments fall off more rapidly than the experimental data. More data are obviously needed at the larger scattering angles in order to reduce the size of the error bars and to better determine the differential-cross-section curve shape.

It should be emphasized that the differential cross sections reported here were normalized to a first-Born-approximation[18] total cross section for excitation of atomic hydrogen to its $n=2$ level at 200 keV. If the normalization were to the particular total $n=2$ excitation cross section at 200 keV obtained from the calculation being compared to experiment, there would be slightly better agreement between the experimental results and that particular theoretical result.

This experiment provides the only measurement of differential cross sections for proton excitation of atomic hydrogen to its $n=2$ level in the energy range 15–145 keV. The agreement between the experimental results and the existing theoretical calculations[28,29,32,33] is reasonably good; however, the differences between the various theories and the experimental data appear to be increasing as the scattering angle increases. The trend in the data suggests that at scattering angles only slightly larger than those reached in this experiment these differences will become significant. Work is in progress in order to extend the angular range of the measurements into the region where the theoretical results appear to diverge. Additional theoretical studies are also needed to extend the understanding of collision processes in the intermediate-energy range.

ACKNOWLEDGMENT

This research was supported in part by the NSF.

---

*Current address: 112 Westbury, Ponca City, Okla. 74601.
†4108 E. Osborn Rd., Phoenix, Ariz. 85018.

[1]J. T. Park, J. E. Aldag, J. L. Peacher, and J. M. George, Phys. Rev. Lett. 40, 1646 (1978).
[2]J. T. Park, J. E. Aldag, and J. M. George, Phys. Rev. Lett. 34, 1253 (1975).
[3]J. T. Park, J. E. Aldag, J. M. George, and J. L. Peacher, Phys. Rev. A 14, 608 (1976).
[4]Y. P. Chong and W. L. Fite, Phys. Rev. A 16, 933 (1977).
[5]J. C. Houver, J. Fayeton, and M. Barat, J. Phys. B 7, 1358 (1974).
[6]T. Kondow, R. J. Girnius, Y. P. Chong, and W. L. Fite, Phys. Rev. A 10, 1167 (1974).
[7]J. T. Morgan, J. Geddes, and H. B. Gilbody, J. Phys. B 6, 2118 (1973).
[8]J. T. Morgan, J. Geddes, and H. B. Gilbody, J. Phys. B 7, 142 (1974).
[9]R. F. Stebbings, R. A. Young, C. A. Oxley, and H. Ehrhardt, Phys. Rev. 138, A1312 (1965).
[10]R. A. Young, R. F. Stebbings, and J. W. McGowan, Phys. Rev. 171, 85 (1968).
[11]J. T. Park, J. M. George, J. L. Peacher, and J. E. Aldag, Phys. Rev. A 18, 48 (1978).
[12]J. T. Park and F. D. Schowengerdt, Rev. Sci. Instrum. 40, 753 (1969).
[13]G. W. York, Jr., J. T. Park, J. J. Miskinis, D. H. Crandall, and V. Pol, Rev. Sci. Instrum. 43, 230 (1972).
[14]F. D. Schowengerdt and J. T. Park, Phys. Rev. A 1, 848 (1970).
[15]V. Pol, W. Kauppila, and J. T. Park, Phys. Rev. A 8, 2990 (1973).
[16]J. T. Park, V. Pol, J. Lawler, J. George, J. Aldag, J. Parker, and J. L. Peacher, Phys. Rev. A 11, 857 (1975).
[17]G. J. Lockwood, H. F. Helbig, and E. Everhart, J. Chem. Phys. 41, 3820 (1964).
[18]D. R. Bates and G. Griffing, Proc. Phys. Soc. London 66, 961 (1953).
[19]M. G. Chidichimo-Frank and D. R. Piacentini, J. Phys. B 7, 548 (1974).
[20]S. K. Knudson and W. R. Thorson, Can. J. Phys. 48, 313 (1970).
[21]C. Gaussorgues, C. LeSech, F. Masnou-Seeuws, R. McCarrol, and A. Riera, J. Phys. B 8, 253 (1975).
[22]I. M. Cheshire, D. F. Gallaher, and A. J. Taylor, J. Phys. B 3, 813 (1970).
[23]D. F. Gallaher and L. Wilets, Phys. Rev. 169, 139 (1968).
[24]D. Rapp and D. Dinwiddie, J. Chem. Phys. 57, 4919 (1972).
[25]D. Rapp, D. Dinwiddie, D. Storm, and T. E. Sharp, Phys. Rev. A 5, 1290 (1972).
[26]L. Wilets and D. F. Gallaher, Phys. Rev. 147, 13 (1966).
[27]E. Everhart, G. Stone, and R. J. Carbone, Phys. Rev. 99, 1287 (1955).
[28]R. Shakeshaft, Phys. Rev. A 18, 1930 (1978). Note that the scale on Fig. 2 is mislabeled. The scattering angle should be in units of 10^{-4} rad.

[29]B. H. Bransden and C. J. Noble, Phys. Lett. A 70, 404 (1979).
[30]J. Callaway and J. W. Wooten, Phys. Rev. A 9, 1294 (1974).
[31]J. Callaway, M. R. C. McDowell, and L. A. Morgan, J. Phys. B 8, 2181 (1975).
[32]V. Franco and B. K. Thomas, Phys. Rev. A 4, 945 (1971).
[33]B. K. Thomas (private communication).